1.0

1.1

1.25 1.4 1.6

2.8 2.5

3.2 2.2

3.6

4.0 2.0

1.8

MICROCOPY RESOLUTION TEST CHART

NATIONAL BUREAU OF STANDARDS 1963 A

(14) NRL-MR-4612

| (9) REPORT DOCUMENTATION PAGE | | READ INSTRUCTIONS BEFORE COMPLETING FORM |
|---|---|---|
| 1. REPORT NUMBER NRL Memorandum Report 4612 | 2. GOVT ACCESSION NO. AD-A107 269 | 3. RECIPIENT'S CATALOG NUMBER |
| 4. TITLE (and Subtitle) (6) THE LOWER-HYBRID-DRIFT INSTABILITY IN NON-ANTIPARALLEL REVERSED FIELD PLASMAS | | 5. TYPE OF REPORT & PERIOD COVERED Interim report on a continuing NRL problem. |
| | | 6. PERFORMING ORG. REPORT NUMBER |
| 7. AUTHOR(s) (10) J. D. Huba, N. T. Gladd*, and J. F. Drake** | | 8. CONTRACT OR GRANT NUMBER(s) |
| 9. PERFORMING ORGANIZATION NAME AND ADDRESS Naval Research Laboratory Washington, DC 20375 | | 10. PROGRAM ELEMENT, PROJECT, TASK AREA & WORK UNIT NUMBERS 61153N; RR033-02-44; 47-0884-0-1 |
| 11. CONTROLLING OFFICE NAME AND ADDRESS (11) 27 | | 12. REPORT DATE October 1981 |
| | | 13. NUMBER OF PAGES 30 (12) 31 |
| 14. MONITORING AGENCY NAME & ADDRESS(if different from Controlling Office) | | 15. SECURITY CLASS. (of this report) UNCLASSIFIED |
| | | 15a. DECLASSIFICATION/DOWNGRADING SCHEDULE |

16. DISTRIBUTION STATEMENT (of this Report)

Approved for public release; distribution unlimited.

16 RR03302
(17) RR033024

17. DISTRIBUTION STATEMENT (of the abstract entered in Block 20, if different from Report)

18. SUPPLEMENTARY NOTES

  *Present address: JAYCOR, San Diego, CA 92138
**Present address: University of Maryland, College Park, MD 20742

19. KEY WORDS (Continue on reverse side if necessary and identify by block number)

| | |
|---|---|
| Lower-hybrid-drift instability | Magnetotail |
| Reversed field plasmas | Magnetic shear |
| Magnetosphere nose | |

20. ABSTRACT (Continue on reverse side if necessary and identify by block number)

The lower-hybrid-drift instability is investigated in non-antiparallel reversed field plasmas, i.e., the magnetic fields on either side of a neutral line are not anti-parallel. Such a magnetic field configuration contains magnetic shear which has a stabilizing influence on the lower-hybrid-drift instability. It is found that magnetic shear has an inhibiting effect on the linear penetration of the lower-hybrid-drift mode toward the neutral line. The implications of this result to the reconnection processes in the magnetosphere (i.e., the nose and the magnetotail) are discussed.

DD FORM 1473 EDITION OF 1 NOV 65 IS OBSOLETE
1 JAN 73
S/N 0102-014-6601

i/ii 251950

# CONTENTS

## THE LOWER-HYBRID-DRIFT INSTABILITY IN NON-ANTIPARALLEL REVERSED FIELD PLASMAS

### I. INTRODUCTION

An important set of problems in plasma physics consists of understanding the physical processes which can occur in reversed field plasmas. For example, how can magnetic field energy be rapidly converted into particle energy? How does the topology of the magnetic field change? Under what conditions can topological changes occur? An enormous amount of work has been devoted to these (and related) questions over the past 20 years. Generally speaking, this research has been focused on the investigation of magnetic field reconnection processes. Some particular topics of interest have been field line annihilation (e.g., 1D Sweet-Parker models); forced reconnection (e.g., 2D Petschek model); and tearing instabilities. In an astrophysical context, this research has been relevant to a variety of space phenomena such as solar flares, interplanetary D sheets and geomagnetic substorms.

One process which can be important in reconnection physics is plasma microturbulence. In general, plasma microinstabilities can often produce anomalous transport of particles, momentum and energy. This can be critical to reconnection process, especially in the null region ($B \simeq 0$), since it allows the plasma to "decouple" from the magnetic field. Moreover, anomalous transport effects can greatly enhance the rate of energy conversion from the magnetic field to the plasma. A variety of microinstabilities which can lead to fine scaled turbulence have been analyzed to determine their relevance to reconnection (see

1

Papadopoulos (1979) for a review). However, a drawback of many of these analyses is the assumption of a one-dimensional magnetic field (i.e., $\underline{B} = B_z(x)\hat{e}_z$); an assumption not usually justified in space plasmas. Other components of the magnetic field leads to the following effects. First, a component of $\underline{B}$ <u>normal to the neutral line</u> (i.e., $\underline{B} = B_x\hat{e}_x + B_z\hat{e}_z$) introduces <u>field line curvature</u>. This effect, which is generally incorporated in micro-instability theories via an artificial gravity, leads to additional particle drifts and can be either a stabilizing or destabilizing influence depending upon the plasma conditions. Secondly, a component of $\underline{B}$ <u>parallel to the current</u> (i.e., $\underline{B} = B_y\hat{e}_y + B_z\hat{e}_z$) introduces <u>magnetic shear</u>. Physically, this corresponds to the situation where the magnetic fields on either side of the neutral are <u>not anti-parallel</u>. Magnetic shear leads to Landau resonances of particles and waves, and the coupling of cross-field modes to parallel propagating modes. Magnetic shear is generally a stabilizing influence on instabilities. Since the magnetic shear induced Landau resonances and parallel mode couplings are strongly dependent on spatial position, the analysis of this effect requires a nonlocal theory. In contrast, the magnetic curvature induced particle drifts are not strongly dependent on spatial position and can be accurately analyzed with a local theory.

In this paper we analyze the effect of magnetic shear on the lower-hybrid-drift instability and discuss some of the implications of magnetic shear as it regards the dynamics of reversed field plasmas in the magnetosphere. We choose the lower-hybrid-

drift instability since it is the most likely instability to be excited in reversed field space plasmas of interest (i.e., the earth's magnetopause and magnetotail (Huba et al., 1978; Gary and Eastman, 1979)). Moreover, the anomalous transport properties associated with this instability can be important to reconnection processes (Huba et al., 1977; Drake et al., 1981; Huba et al., 1980). We focus here on the effect of magnetic shear on the lower-hybrid-drift instability since it has been shown to have a strong stabilizing effect on this mode [ Krall, 1978]. We will not consider here the effect of field line curvature since it has a much weaker influence on the lower-hybrid-drift instability (Krall and McBride, 1977; Rajal and Gary, 1981).

A self-consistent theory of the lower-hybrid-drift instability in a sheared, reversed field plasma is difficult to develop. Major complications arise because of finite plasma $\beta$ and electron temperature effects (i.e., electromagnetic coupling, electron $\nabla B$ drift-wave resonance, finite electron Larmor radius effects). The inclusion of these effects, within the context of a weakly nonlocal stability analysis, leads to three coupled, partial differential equations involving complex velocity integrations. At this early stage of analysis, we do not attempt such a comprehensive theory. Rather, we use a simpler theory here to examine the dominant effect of magnetic shear on the lower-hybrid-drift instability with emphasis on understanding the implications of this mode for reversed field plasma dynamics. Specifically, we simplify the analysis by using electrostatic theory with cold electrons. However, we do include an Appendix which

3

discusses the effect of electromagnetic coupling and electron $\nabla B$ drift-wave resonances in the shear stabilization criterion. A more comprehensive theory will be presented in a future report.

The scheme of the paper is as follows. In Section II we present a general discussion of the lower-hybrid-drift instability and the effect of magnetic shear on it; showing specific results of our analysis, i.e., a marginal stability curve showing the stabilizing influence of shear. We also apply these results to a particular sheared, reversed magnetic field configuration. In Section III we discuss the implications of these results on reconnection processes in the earth's magnetosphere. Finally, an analysis incorporating finite $\beta$ effects is presented in the Appendix.

## II. THEORY

### A. Assumptions and Plasma Configuration

The plasma configuration and slab geometry we consider is described as follows. The ambient magnetic field is in the y-z plane ($\underset{\sim}{B} = B_y\hat{e}_y + B_z\hat{e}_z$) and is only a function of x. The density is also a function of x but we take the ion temperature to be finite and constant. For simplicity, we take the electron temperature to be zero (i.e., $T_e/T_i \rightarrow 0$). Finite electron temperature effects are discussed in the Appendix. Equilibrium force balance on an ion fluid element in the x direction requires $V_{iy}=V_{di}$ where $V_{di} = (v_i^2/2\Omega_i) \partial \ln n/\partial x$ is the ion diamagnetic drift velocity. Here, $v_i = (2T_i/m_i)^{\frac{1}{2}}$ is the ion thermal velocity and $\Omega_i = eB_0/m_i c$ is the ion Larmor frequency. We can relate the ion diamagnetic velocity to the mean ion Larmor radius and scale length of the density gradient by $V_{di}/v_i = r_{Li}/2L_n$ where $r_{Li} = v_i/\Omega_i$ and $L_n = (\partial \ln n/\partial x)^{-1}$. The electrons are assumed to be magnetized, while the ions are treated as unmagnetized. This is reasonable since, in treating the lower-hybrid-drift instability, we are considering waves such that $\Omega_i \ll \omega \ll \Omega_e$ and $k^2 r_{Li}^2 \gg 1$. Only electrostatic oscillations are considered (electromagnetic coupling is discussed in the Appendix) and we assume that the plasma is weakly inhomogeneous in the sense that $r_{Le}^2 (\partial \ln n/\partial x)^2 \ll 1$ and $r_{Le}^2 (\partial \ln B/\partial x)^2 \ll 1$. We assume that the local equilibrium magnetic field is

$$\underset{\sim}{B}(x) = B_0(x_0)(\hat{e}_z + (x-x_0)/L_s\hat{e}_y) \tag{1}$$

in the vicinity of $x = x_0$ (i.e., $(x-x_0)/L_s \ll 1$) where

5

$L_s = (\partial \phi / \partial x)^{-1}$ and $\phi = \tan^{-1}(B_y B_z)$. Thus, $L_s$ is the scale length characterizing the magnetic shear.

If, for the moment, we consider $\underline{B} = B_o e_z$, then the plasma configuration just described is unstable to the kinetic lower-hybrid-drift instability when $1 > V_{di}/v_i > (m_e/m_i)^{\frac{1}{2}}$ (Davidson et al., 1977). The instability is driven by the cross-field current and is excited via an ion-wave resonance (i.e., inverse Landau damping). The waves are characterized at maximum growth by $\omega_r \sim k_y V_{di} \lesssim \omega_{\ell h}$, $\gamma \lesssim \omega_r$, $k_y \rho_{es} \simeq 1$ and $\underset{\sim}{k} \cdot \underset{\sim}{B} = 0$ where $\rho_{es} = (T_i/m_e)^{\frac{1}{2}}/\Omega_e$. For modes such that $\underset{\sim}{k} \cdot \underset{\sim}{B} \neq 0$ (i.e., $k_{\parallel} \neq 0$), electron Landau damping reduces their growth rate or stabilizes them, depending on the magnitude of $k_{\parallel}$. We now let $\underset{\sim}{B} = B_y(x)\hat{e}_y + B_z\hat{e}_z$ as in Eq. (1), which introduces magnetic shear as shown in Fig. 1. The magnetic field rotates in the y-z plane as a function of x so that $k_{\parallel}$ is also a function of x. At $x = x_o$ we note that $k_{\parallel} = 0$ ($\underset{\sim}{k} \cdot \underset{\sim}{B} = 0$) but at $x = x_1$, $k_{\parallel} \neq 0$ ($\underset{\sim}{k} \cdot \underset{\sim}{B} \neq 0$). Thus, the dispersive properties of the plasma are also a function of x (e.g., electron Landau damping and parallel mode coupling can occur at $x_1$ but not at $x_o$). Making use of Eq. (1), we use the prescription $k_z(x) = k_{zo} + k_y (x-x_o)/L_s$ to incorporate magnetic shear into the analysis where we choose $k_{zo} = k_z(x=x_o) = 0$.

B. Dispersion Equation

Within the context of the assumptions outlined in the previous sub-section, the equation which describes the lower-hybrid-drift instability in a sheared magnetic field is given by [Davidson et al., 1978].
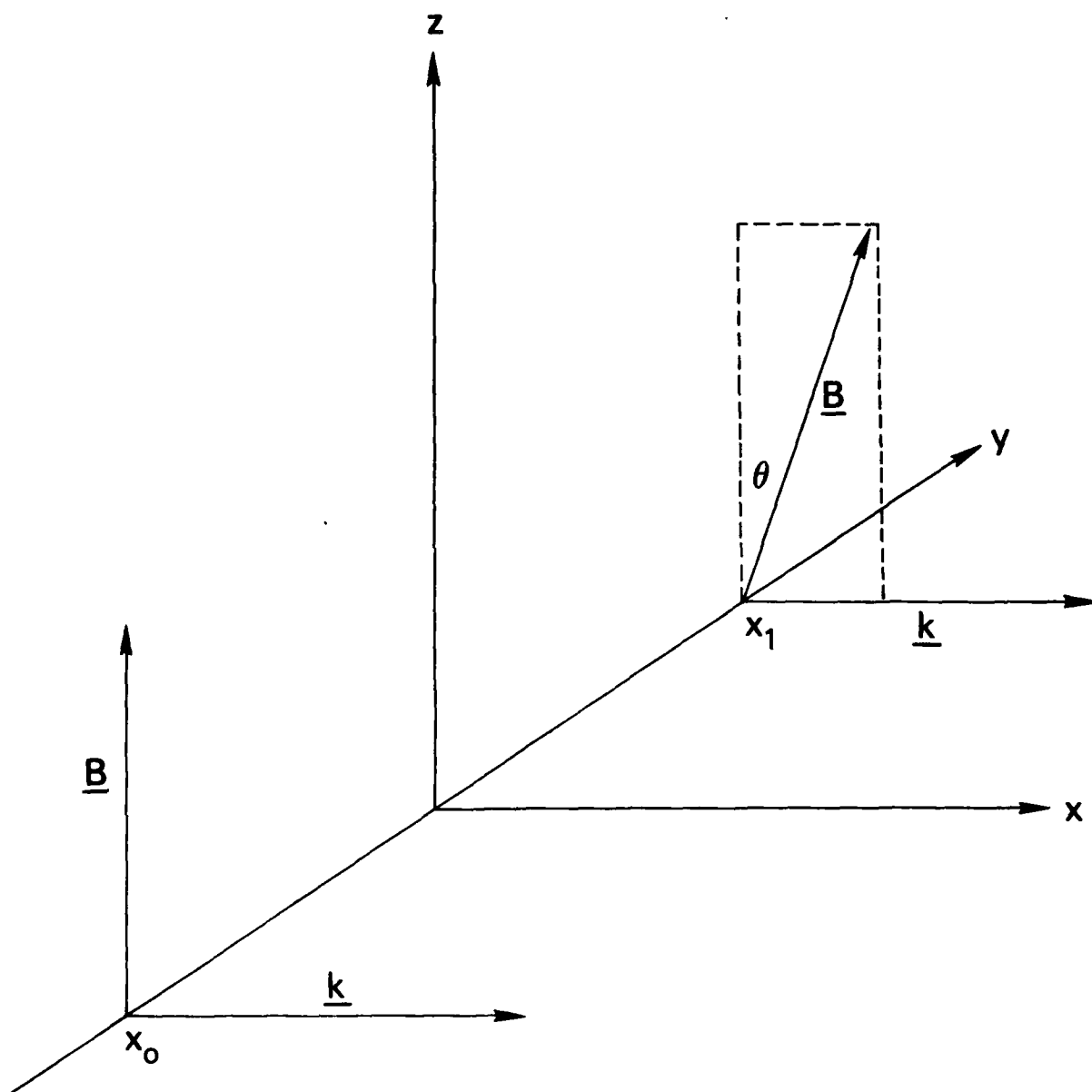
Fig. 1 — Geometry of sheared magnetic field

$$A \frac{\partial^2 \phi}{\partial x^2} + \left[B - C(x-x_o)\right]^2 \phi = 0 \qquad (2)$$

where

$$k_y^2 A = - \frac{2\omega_{pi}^2}{k^2 v_i^2} \left[k^2 \rho_{es}^2 - Z''(\zeta_i)\right] \qquad (3)$$

$$B = \frac{2\omega_{pi}^2}{k^2 v_i^2} \left[k^2 \rho_{es}^2 - \frac{kV_{di}}{\omega} + 1 + \zeta_1 Z(\tau_i)\right] \qquad (4)$$

$$C = \frac{\omega_{pe}^2}{\omega^2} \frac{1}{L_s^2} \qquad (5)$$

and $\omega_{p\alpha}^2 = 4\pi n e^2/m_\alpha$, $v_i^2 = 2T_i/m_i$, $\rho_{es}^2 = (T_i/m_e\Omega_e^2)$, $V_{di} = (v_i^2/2\Omega_i)\partial \ln n/\partial x$ and $\zeta_i = (\omega - k_y V_{di})/kv_i$. In writing Eq. (2) we have assumed $k^2\lambda_D^2 \ll 1$ and $\omega_{pe}^2 \gg \Omega_e^2$ where $\lambda_D^2 = v_i^2/2\omega_{pi}^2$.

Equation (2) is in the form of Weber's equation and the eigenfrequency is defined by

$$B = (2m + 1)(AC)^{\frac{1}{2}} \qquad (6)$$

where m is the mode number (i.e., m = 0, 1, 2, ...). The branch is chosen according the outgoing energy prescription of Pearlstein and Berk (1969). The associated eigenfunction is

$$\phi = \phi_o H_m(\alpha x) \exp[-\alpha^2 x^2/2] \qquad (7)$$

where $\alpha = (C/A)^{\frac{1}{4}}$ and $H_m$ is the Hermite polynominal of order m. In general, a numerical analysis is required to solve Eq. (6) (using Eqs. (3)-(5)). However, we first consider a limiting case to obtain an analytical solution to Eq. (6).

8

We consider the weak drift limit, $V_{di} \ll v_i$, so that the Z functions in Eqs. (3) and (4) can be approximated by $Z(\zeta_i) \simeq i\sqrt{\pi}$. The dispersion equation then becomes

$$D(\omega,k) = 1 + k^2 \rho_{es}^2 - \frac{k_y V_{di}}{\omega} + i\left[ \sqrt{\pi}\left(\frac{\omega - k_y V_{di}}{k v_i}\right) + \frac{1}{k\lambda_{di}}\frac{\omega_{pe}}{\omega}\frac{1}{k_y L_s}\right.$$

$$\left. k \rho_{es} \; (2m + 1)\right] = 0 \qquad (8)$$

The first imaginary term is a destabilizing term due to inverse ion Landau damping. The second imaginary term is the stabilizing effect of magnetic shear. It's origin in the analysis is a term $\propto (\frac{k_\parallel}{\omega})^2$ in the magnetized electron response. Physically, magnetic shear leads to stabilization since it allows wave energy to propagate away from the excitation region (i.e., where $k_\parallel = 0$).
The real frequency is given by

$$\omega_r = k V_{di}/(1 + k^2 \rho_{es}^2) \qquad (9)$$

where shear corrections to $\omega_r$ have been neglected. The mode is stabilized when $\mathrm{Im}\, D(\omega,k) = 0$ or

$$\left(\frac{L_n}{L_s}\right)_{cr} = \frac{\sqrt{\pi}}{(2m+1)}\frac{V_{di}}{v_i}\frac{k^2\rho_{es}^2}{(1+k^2\rho_{es}^2)^2} \qquad (10)$$

where Eq. (9) has been used and the subscript cr refers to the critical value of $L_n/L_s$. The maximum value of the RHS of Eq. (10) occurs for $k^2\rho_{es}^2 = 1.0$ so that all wavenumbers are stable when

$$\frac{L_n}{L_s} > \frac{\sqrt{\pi}}{4}(2m+1)^{-1}\frac{V_{di}}{v_i}\left(\text{or} > \frac{\sqrt{\pi}}{8}(2m+1)^{-1}\frac{r_{Li}}{L_n}\right) \qquad (11)$$

9

Note that the higher order modes ($m \neq 0$) are more easily stabilized by shear than the lowest order mode ($m = 0$) (i.e., $L_s(m \neq 0) > L_s(m = 0)$).

We now relax the weak drift assumption and solve Eq. (6) numerically. Figure (2) is a plot of $(L_n/L_s)_{cr}$ vs. $V_{di}/v_i$ for $\omega_{pe}^2/\Omega_e^2 = 100$, $\beta = 0.0$, $m = 0$ and $T_e = 0$. The growth rate is maximized with respect to $k\rho_{es}$ so that the maximum value of $(L_n/L_s)_{cr}$ necessary to stabilize the mode is obtained. Two regions are labeled: stable $(L_n/L_s > (L_n/L_s)_{cr})$ and unstable $(L_n/L_s < (L_n/L_s)_{cr})$. For $V_{di}/v_i = 1.0$ we find that $(L_n/L_s)_{cr} = 0.325$ which, surprisingly, is in good agreement with our analytical result [Eq. (11)] even though the drift is not weak.

### C.  Application to Reversed Field Plasmas

In order to apply these results to a reversed field plasma, we consider the following magnetic field profile

$$\underset{\sim}{B} = B_o \left[ \sin \frac{\theta}{2} \, \hat{e}_y + \cos \frac{\theta}{2} \tanh \frac{x}{\lambda} \, \hat{e}_z \right] \qquad (12)$$

Equation (12) describes a reversed field plasma (i.e., the z-component reverses direction at $x = 0$) with the field undergoing a total directional change $\pi + \theta$ in the y-z plane. Thus, if $\theta = 0$ then the standard one-dimensional Harris profile is recovered (i.e., anti-parallel field) with a discontinuous rotation at $x = 0$. On the other hand, for $\theta \neq 0$ the field con-tinuously rotates in the y-z plane and remains finite every-where. This profile (Eq. (12)) is a rough approximation to the

10
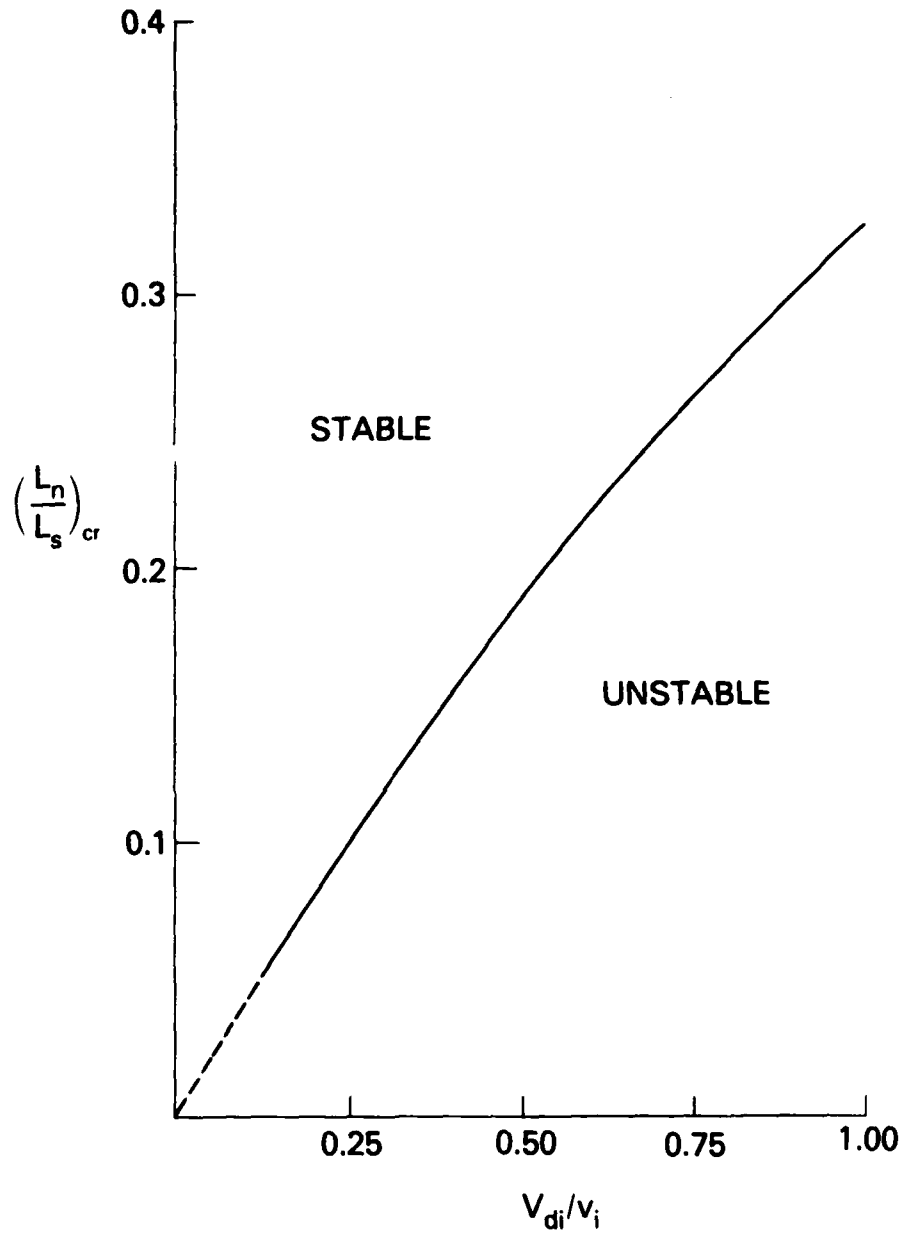
Fig. 2 — Plot of $(L_n/L_s)$cr vs. $V_{di}/v_i$ for $\omega_{pe}^2/\Omega_e^2 = 100$ and $T_e = 0$. The lower-hybrid-drift instability is stable (unstable) for $L_n/L_s > (L_n/L_s)_{cr}$ ($L_n/L_s < (L_n/L_s)_{cr}$). The curve is dashed for $V_{di}/v_i < (m_e/m_i)^{1/4} \approx 0.16$ because the ions are magnetized in this regime and our theory, strictly speaking, is not applicable.

11

magnetic field of the nose of the magnetosphere of the earth.
It also approximates the distant geomagnetic tail when no normal
field component is present.

We plot $L_n/L_s$ vs. $x/\lambda$ for several values of $\theta$ ($\theta$ = 5°, 10°,
15°, 20°, 25°, 30°, 45°) in Figure 3. We note that $L_n/L_s$ varies
2-3 orders of magnitude over the range of $x/\lambda$ shown. Also, as $\theta$
increases so does $L_n/L_s$, as anticipated. In the region
$x/\lambda \leqslant 0.25$, the shear is strong (i.e., $L_s \geqslant L_n$) and the theory
discussed in this paper is not adequate. Thus, we restrict
our attention to regions such that $L_n > L_s$.

We combine the results of Figs. (2) and (3) in Fig. 4
which plots $\theta$ vs. $x_p/\lambda$ for several values of $V_{di}/v_i$ ($V_{di}/v_\perp$ = 0.25
0.50, 1.00 which correspond to $\lambda/r_{Li}$ = 4.0, 2.0, 1.0, respectively).
Here, $x_p/\lambda$ represents the <u>linear</u> penetration distance of the
lower-hybrid-drift instability. That is, we expect the modes to
be stable for $x < x_p$ because of shear stabilization. We find
that (1) as the ion diamagnetic drift increases (i.e., the cur-
rent sheet becomes thinner) the mode can penetrate closer to the
"null" region (i.e., $x \simeq 0$) and (2) as $\theta$ increases, which
increases the magnetic shear, the penetration distance $x_p/\lambda$
becomes larger. Nonlocal analysis of the lower-hybrid-drift
instability in a field reversed plasma (Huba et al., 1980) has
found that the dominant mode is localized at a position
$x/\lambda \simeq 1.25$ for $T_e$ = 0. Thus, even for $\theta$ = 45° the fastest
growing mode is not stabilized due to shear. However, higher
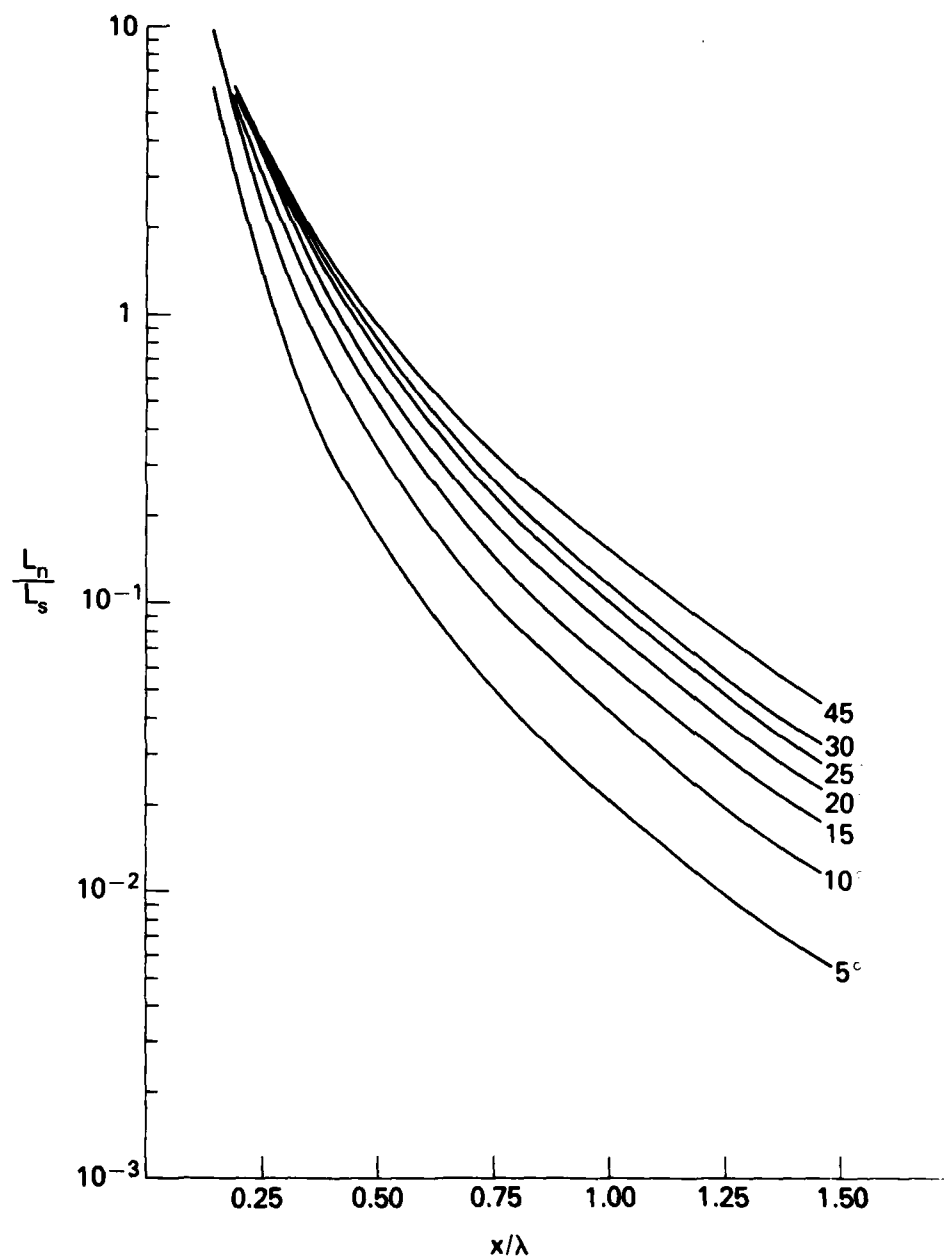order modes, which penetrate closer to $x$ = 0, are expected to be

12

Fig. 3 — Plot of $L_n/L_s$ vs. $x/\lambda$ for the magnetic field profile given by Eq. (12) and several values of $\theta$. Note that the shear parameter $L_n/L_s$ varies over 3 orders of magnitude.

13
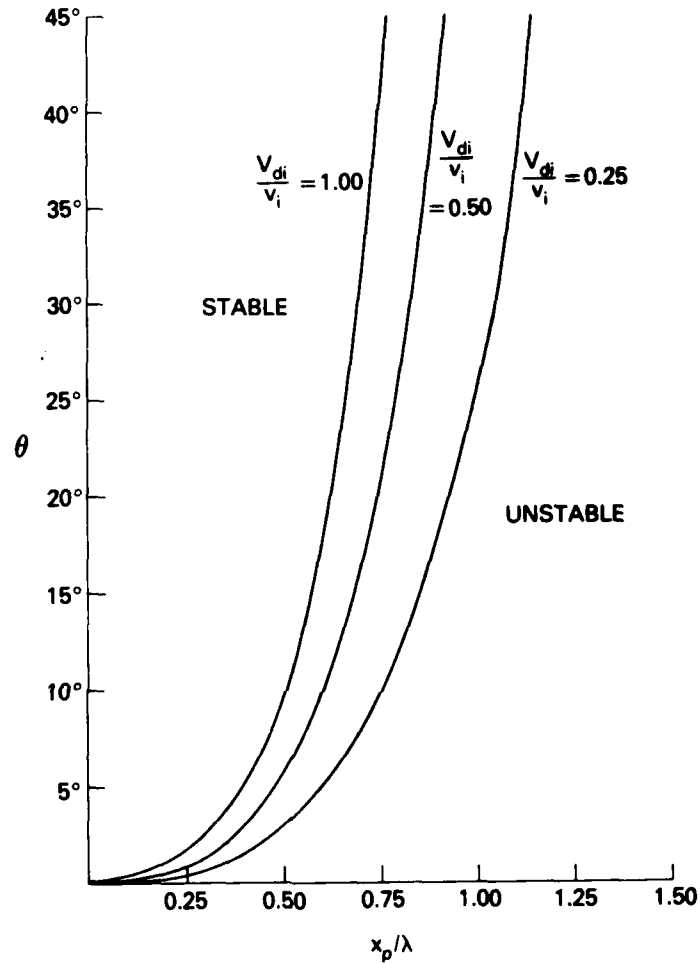
Fig. 4 — Plot of $\theta$ vs. $x_p/\lambda$ for $V_{di}/v_i$ = 1.00, 0.50, 0.25.  Here, $\theta$ represents the strength of the magnetic shear in a reversed field plasma (i.e., $\theta = 0$:  no shear, fields anti-parallel; $\theta \neq 0$:  shear, fields non-antiparallel) and $x_p/\lambda$ is the linear penetration distance of the lower-hybrid-drift instability to the neutral line. The mode is linearly stable (unstable) in the region $x < x_p$ ($x > x_p$).  As the amount of shear increases, i.e., $\theta$ becomes larger, the mode is stabilized further away from the neutral line ($x = 0$).

14

affected by shear.  These results are, however, highly profile dependent.  If the dominant shearing of the field occurred in the region where the LHD was localized, rather than in the null region (the situation implied by Eq. (12)), then the stabilizing effect of shear would be much more pronounced.

## III. DISCUSSION

The purpose of this brief report has been to study the influence of magnetic shear on the lower-hybrid-drift instability in reversed field plasmas. As mentioned in the introduction, microturbulence associated with such modes can play an important role in the dynamic evolution of a reversed field plasma via its anomalous transport properties. The lower-hybrid-drift instabiltiy, although linearly stable in the field reversal region near the neutral line (Huba et al., 1980), does play a dramatic role in the evolution of an anti-parallel field reversed plasma (Drake et al., 1981; Winske, 1981; Tanaka and Sato, 1981). It has been shown both theoretically and by computer simulations that the mode causes magnetic flux to diffuse <u>towards</u> the neutral line which leads to an enhanced current density at the neutral line. Eventually microturbulence penetrates to the null region and permits field line reconnection/annihilation to occur, thereby dissipating magnetic energy. In the case where the reversed field is non-antiparallel (i.e., the field is sheared) we have found here that the lower-hybrid-drift instability will be linearly unstable further away from the neutral line than the case where the field is completely anti-parallel (Fig. 4). Thus, magnetic shear has an inhibiting effect on the penetration of the lower-hybrid-drift mode toward the neutral line. We anticipate that this means that the evolution of a non-antiparallel reversed field plasma will differ from that of an anti-parallel one. For example, if the shear is sufficiently strong the mode

16

may take substantially longer to penetrate to the neutral line
or may not penetrate at all.  This conjecture, of course, is
based on our linear analysis and must be substantiated by further
(nonlinear) analysis.  Also, we reemphasize that the results
presented in this paper are not comprehensive since we have
neglected important finite $\beta$ and $T_e$ effects (i.e., coupling of
electromagnetic and electrostatic fluctuations and $\nabla B$ resonances).
Nonetheless, our results are qualitatively correct although they
can be improved quantitatively.  We are presently developing
a more comprehensive theory for finite $\beta$ and $T_e$ plasmas and
will report our results in a future publication.

Two regions of the magnetosphere in which the magnetic
field can reverse direction (in one component) and is also sheared
are the nose and magnetotail.  In both these regions reconnection
processes are believed to occur and can be important to the dyna-
mic interaction of the solar wind and the magnetosphere.  In the
case of the nose, the angle between the incoming IMF and the
earth's geomagnetic field varies from $0$ to $\pi$.  A thin magneto-
pause boundary layer exists (whose width is roughly $r_{Li}$) over
which the $\underline{B}$ field undergoes a directional change.  In the magne-
totail it is known that a substantial crosstail magnetic field
($B_y \lesssim 15\gamma$) can exist at times [Akasofu et al., 1978].  Such a
magnetic field can introduce a strong shear, i.e., the magnetic
field undergoes a rotation as one passes from the north to south
lobe.

Crooker (1978) has suggested that the nose reconnection only

17

occurs in regions where the IMF and geomagnetic field are anti-parallel (no shear). Classical reconnection theories predict reconnection even if the fields are non-antiparallel [Ugai, 1981] so that some "anomalous" process may be responsible for inhibiting reconnection in this instance. Moreover, for reconnection events observed at the nose, the time scale for the energization of the plasma appears to be slower for more strongly sheared cases (non-antiparallel fields) than for non-sheared fields (anti-parallel fields) (Russell, private communication). We suggest one possibility for such an effect is the influence of magnetic shear on the lower-hybrid-drift instability (or other instabilities) and its associated microturbulence.

## ACKNOWLEDGMENTS

# APPENDIX

We derive an expression for $(L_n/L_s)_{cr}$ which includes finite $\beta$ effects (i.e., electrostatic-electromagnetic coupling, electron $\nabla B$ drift-wave resonance). In order to make the analysis tractable, we consider the limit $\beta_i \ll 1$ and $T_e \ll T_i$. The nonlocal dispersion equation is given by [Davidson et al., 1977]

$$A \frac{\partial^2 \phi}{\partial x^2} + [B - C(x-x_o)^2]\phi = 0 \tag{A1}$$

where

$$A = -\frac{1}{k_y^2} \frac{\omega_{pe}^2}{\Omega_e^2} \tag{A2}$$

$$B = \frac{2\omega_{pi}^2}{k^2 v_i^2}\left[1 + k^2\rho_{es}^2\left(1 + \frac{\omega_{pe}^2}{c^2 k^2}\right) - \frac{kV_{di}}{\omega}\left(1 + \frac{\beta_i}{2}\right)\right.$$

$$\left. + i\zeta_i\sqrt{\pi} + i\frac{\pi}{2}\frac{T_i}{T_e}J_o^2\left(\frac{kv_r}{\Omega_e}\right)s_e\exp(-s_e)\right] \tag{A3}$$

$$C = \frac{\omega_{pe}^2}{\omega^2}\frac{1}{L_s^2}\left(1 + \frac{\omega_{pe}^2}{c^2 k^2}\right)^{-1} \tag{A4}$$

where $\omega_{p\alpha}^2 = 4\pi n e_\alpha^2/m_\alpha$, $v_\alpha^2 = 2T_\alpha/m_\alpha$, $\rho_{es}^2 = (T_i/m_e)/\Omega_e^2$, $\beta_i = 8\pi n T_i/B^2$, $V_{di} = (v_i^2/2\Omega_i)\partial \ln n/\partial x$, $s_e = v_r^2/v_e^2$, $\rho_i = (\omega - kV_{di})/kv_i$, $v_r^2 = 2\Omega_e\omega_r/k_y\epsilon_B$ and $\epsilon_B = \partial \ln B/\partial x$. The finite $\beta$ corrections included in (A1) are as follows. First, the coupling of electromagnetic and electrostatic perturbations arises from terms proportional to $\omega_{pe}^2/c^2 k^2$. The $\beta$ dependence can be seen by

noting that $k^2\rho_{es}{}^2(\omega_{pe}{}^2/c^2k^2) = \beta_i/2$. Second, non-resonant electron $\nabla B$ effects are contained in the term proportional to $\beta_i(kV_{di}/\omega)$. This is a fluid-like response of the electrons due to the inhomogeneous magnetic field. Finally, resonant electron $\nabla B$ effects are contained in the final term of B in Eq. (A2). Equations (A2)-(A4) are similar to those derived by Davidson et al. (1977) but, in addition, contain electron resonance terms (Huba and Wu, 1977).

We now assume $kv_r/\Omega_e \gg 1$ which corresponds to $\beta_i \ll k^2\rho_{es}{}^2 \sim 1$ and rewrite Eqs. (A2) - (A4) as follows

$$A = - \frac{1}{k_y{}^2} \frac{\omega_{pe}{}^2}{\Omega_e{}^2} \tag{A5}$$

$$B = \frac{2\omega_{pi}{}^2}{k^2v_i{}^2} \left[ k^2\rho_{es}{}^2 + \left(1 - \frac{kV_{di}}{\omega}\right) \left(1 + \frac{\beta_i}{2}\right)\right.$$
$$\left. + i\sqrt{\pi} \; \frac{\omega}{kv_i} \left(1 - \frac{kV_{di}}{\omega}\right) + \frac{T_i}{T_e} \left(\frac{\beta_i}{2}\right)^{\frac{1}{2}} s_e \exp(-s_e)\right] \tag{A6}$$

$$C = \frac{\omega_{pe}{}^2}{\omega^2} \frac{1}{L_s{}^2} \left(1 + \frac{\beta_i}{2k^2\rho_{es}{}^2}\right)^{-1} \tag{A7}$$

The dispersion equation is again given by Eq. (1). The real frequency is the same as Eq. (9) but with $\hat{\rho}_{es}$ replacing $\rho_{es}$ where $\hat{\rho}_{es} = \rho_{es}/(1 + \beta_i/2)$. To lowest order in $\beta_i$, the critical shear length is

$$\left(\frac{L_n}{L_s}\right)_{cr} = \sqrt{\pi}\,\frac{V_{di}}{v_i}\,\frac{k^2\hat{\rho}_{es}^2}{1+k^2\hat{\rho}_{es}^2}\left(1 + \frac{\beta_i}{4k^2\rho_{es}^2}\right) - \frac{T_i}{T_e}\left(\frac{\beta_i}{2}\right)^{\frac{1}{2}}\frac{s_e\exp(-s_e)}{1+k^2\hat{\rho}_{es}^2}$$

(A8)

where $s_e$ can be written as

$$s_e = \frac{2}{\beta_e}\,\frac{1}{1+k^2\hat{\rho}_{es}^2}$$

(A9)

Maximizing $(L_n/L_s)_{cr}$ with respect to wavenumber yields

$$\left(\frac{L_n}{L_s}\right)_{cr} = \frac{\sqrt{\pi}}{4}\,\frac{V_{di}}{v_i}\left(1 + \frac{\beta_i}{4}\right) - \frac{1}{2}\left(\frac{T_i}{T_e}\right)^2\frac{\exp(-1/\beta_e)}{(2\beta_i)^{\frac{1}{2}}}$$

(A10)

where $k\rho_{es} \simeq k\hat{\rho}_{es} = 1$.

Two interesting points concerning Eqs. (A7) and (A9) are the following. First, the finite $\beta_i$ dependence in the first term of Eqs. (A7) and (A9) arise from the electromagnetic correction due to $\delta A_\parallel$ (i.e., the transverse magnetic field fluctuations). The influence of this correction is to increase the amount of shear necessary to stabilize the mode (Davidson et al., 1978). That is, as $\beta_i$ increases then the shear length $L_s$ necessary for stabilization decreases so that the mode is harder to stabilize. Physically this occurs because the fluctuating electric field associated with $\delta A_\parallel$ inhibits free streaming electron flow along the magnetic field which reduces the rate at which energy can be convected away from the localization region (Pearlstein and Berk, 1969). Secondly, the second term in Eq. (A8) represents the resonant $\nabla B$ correction which is a

21

damping effect. This term tends to <u>decrease</u> the amount of shear necessary to stabilize the mode. Thus, the finite $\beta$ corrections have different influences on the shear stabilization criterion. Loosely speaking, electromagnetic effects are destabilizing (i.e., a stronger shear is needed to stabilize the mode from the $\beta = 0$ situation) while the resonant $\nabla B$ effects are stabilizing (i.e., a weaker shear is needed to stabilize the mode from the $\beta = 0$ situation). As to which effect dominates, a more careful analysis is needed which we are presently developing and will be presented in a future report.

# REFERENCES

Akasofu, S.-I., A.T.Y. Lui, C.I. Meng and M. Haurwitz, Need
for a three-dimensional analysis of magnetic fields in the
magnetotail during substorms, Geophys. Res. Lett. 5, 283,
1978.

Crooker, N.U., The half-wave rectifier response of the magneto-
sphere and anti-parallel merging, J. Geophys. Res. 85,
575, 1980.

Davidson, R.C., N.T. Gladd and Y. Goren, Influence of magnetic
shear on the lower-hybrid-drift instability in toroidal
reversed-field plasmas, Phys. Fluids 21, 992, 1978.

Drake, J.F., N.T. Gladd and J.D. Huba, Magnetic field diffusion
and dissipation in reversed field plasmas, Phys. Fluids
24, 78, 1981.

Gary, S.P. and T.E. Eastman, The lower-hybrid-drift instability
at the magnetopause, J. Geophys. Res. 84, 7378, 1979.

Huba, J.D. and C.S. Wu, Effects of a magnetic field gradient
on the lower-hybrid-drift instability, Phys. Fluids 19,
988, 1976.

Huba, J.D., N.T. Gladd and K. Papadopoulos, The lower-hybrid-
drift instability as a source of anomalous resistivity for
magnetic field line reconnection, Geophys. Res. Lett. 4,
125, 1977.

Huba, J.D., N.T. Gladd and K. Papadopoulos, Lower-hybrid-drift
wave turbulence in the distant magnetotail, J. Geophys. Res.
83, 5217, 1978.

Huba, J.D., J.F. Drake and N.T. Gladd, Lower-hybrid-drift instability in field reversed plasmas, Phys. Fluids 23, 552, 1980.

Huba, J.D., N.T. Gladd and J.F. Drake, On the role of the lower-hybrid-drift instability in substorm dynamics, to be published in J. Geophys. Res., 1981.

Krall, N.A. and J.B. McBride, Magnetic curvature and ion distribution function effects on lower-hybrid-drift instabilities, Phys. Fluids 19, 1970, 1976.

Krall, N.A., Shear stabilization of lower-hybrid-drift instabilities, Phys. Fluids 20, 311, 1977.

Pearlstein, L.D. and H.L. Berk, Universal eigenmode in a strongly sheared magnetic field, Phys. Rev. Lett. 23, 220, 1969.

Rajal, L.J. and S.P. Gary, The lower-hybrid-drift density drift instability with magnetic curvature, submitted to Phys. Fluids, 1981.

Tanaka, M. and T. Sato, Simulations in lower-hybrid-drift instability and anomalous resistivity in magnetic neutral sheet, to be published in J. Geophys. Res., 1981.

Ugai, M., Magnetic field reconnection in a sheared field, J. Plasma Phys. 25, 89, 1981.

Winske, D., Current-driven microinstabilities in a neutral sheet, Phys. Fluids,   , 1981.

Director
Naval Research Laboratory
Washington, D.C. 20375
　　　Attn:　T. Coffey (26 copies)
　　　　　　 J. Brown
　　　　　　 S. Ossakow (100 copies)

University of Alaska
Geophysical Institute
Fairbanks, Alaska 99701
　　　Attn:　Library

University of Arizona
Dept. of Planetary Sciences
Tucson, Arizona 85721
　　　Attn:　J. R. Jokipii

University of California, S. D.
LaJolla, California 92037
　(Physics Dept.):
　　　Attn:　J. A. Fejer
　　　　　　 T. O'Neil
　　　　　　 Vu Yuk Kuo
　　　　　　 J. Winfrey
　　　　　　 Library
　　　　　　 J. Malmberg
　(Dept. of Applied Sciences):
　　　Attn:　H. Booker

University of California
Los Angeles, California 90024
　(Physics Dept.):
　　　Attn:　J. M. Dawson
　　　　　　 B. ·ried
　　　　　　 J. G. Moralles
　　　　　　 Y. Lee
　　　　　　 A. Wong
　　　　　　 F. Chen
　　　　　　 Library
　　　　　　 R. Taylor
　(Institute of Geophysics and
　 Planetary Physics):
　　　Attn:　Library
　　　　　　 C. Kennel
　　　　　　 F. Coroniti

Columbia University
New York, New York 10027
　　　Attn:　R. Taussig
　　　　　　 R. A. Gross

University of California
Berkeley, California 94720
　(Space Sciences Laboratory):
　　　Attn:　Library
　　　　　　 M. Hudson
　(Physics Dept.):
　　　Attn:　Library
　　　　　　 A. Kaufman
　　　　　　 C. McKee
　(Electrical Engineering Dept.):
　　　Attn:　C. K. Birdsall

University of California
Physics Department
Irvine, California 92664
　　　Attn:　Library
　　　　　　 G. Benford
　　　　　　 N. Rostoker
　　　　　　 C. Robertson
　　　　　　 N. Rynn

California Institute of Technology
Pasadena, California 91109
　　　Attn:　R. Gould
　　　　　　 L. Davis, Jr.
　　　　　　 P. Coleman

University of Chicago
Encrico Fermi Institute
Chicago, Illinois 60637
　　　Attn:　E. N. Parker
　　　　　　 I. Lerche
　　　　　　 Library

University of Colorado
Dept. of Astro-Geophysics
Boulder, Colorado 80302
　　　Attn:　M. Goldman
　　　　　　 Library

Cornell University
Laboratory for Plasma Physics
Ithaca, New York 14850
　　　Attn:　Library
　　　　　　 R. Sudan
　　　　　　 B. Kusse
　　　　　　 H. Fleischmann
　　　　　　 C. Wharton
　　　　　　 F. Morse
　　　　　　 R. Lovelace

Harvard University
Cambridge, Massachusetts 02138
    Attn:  Harvard College
           Observatory (Library)
           G. S. Vaina
           M. Rosenberg

Harvard University
Center for Astrophysics
60 Garden Street
Cambridge, Massachusetts 02138
    Attn:  G. B. Field

University of Iowa
Iowa City, Iowa 52240
    Attn:  C. K. Goertz
           G. Knorr
           D. Nicholson

University of Houston
Houston, Texas 77004
    Attn:  Library

University of Michigan
Ann Arbor, Michigan 48104
    Attn:  E. Fontheim

University of Minnesota
School of Physics
Minneapolis, Minnesota 55455
    Attn:  Library
           J. R. Winckler
           P. Kellogg

M.I.T.
Cambridge, Massachusetts 02139
    Attn:  Library
 (Physics Dept.):
    Attn:  B. Coppi
           V. George
           G. Bekefi
           T. Dupree
           R. Davidson
 (Elect. Engineering Dept.):
    Attn:  R. Parker
           A. Bers
           L. Smullin
 (R. L. E.):
    Attn:  Library
 (Space Science):
    Attn:  Reading Room

Northwestern University
Evanston, Illinois 60201
    Attn:  J. Denevit

Princeton University
Princeton, New Jersey 08540
    Attn:  Physics Library
           Plasma Physics Lab. Library
           M. Rosenbluth
           C. Oberman
           F. Perkins
           T. K. Chu
           V. Aranasalan
           H. Hendel
           R. White
           R. Kurlsrud
           H. Furth
           M. Gottlieb
           S. Yoshikawa
           P. Rutherford

Rice University
Houston, Texas 77001
    Attn:  Space Science Library
           R. Wolf

University of Rochester
Rochester, New York 14627
    Attn:  A. Simon

Stanford University
Institute for Plasma Research
Stanford, California 94305
    Attn:  Library
           F. W. Crawford

Stevens Institute of Technology
Hoboken, New Jersey 07030
    Attn:  B. Rosen
           G. Schmidt
           M. Seidl

University of Texas
Austin, Texas 78712
    Attn:  W. Drummond
           V. Wong
           D. Ross
           W. Horton
           D. Choi
           R. Richardson
           G. Leifeste

College of William and Mary
Williamsburg, Virginia 23185
    Attn:  F. Crownfield

Lawrence Livermore Laboratory
University of California
Livermore, California 94551
    Attn:  Library
           B. Kruer
           J. Thomson
           J. Nucholls
           J. DeGroot
           L. Wood
           J. Emmett
           B. Lasinsky
           B. Langdon
           R. Briggs
           D. Pearlstein

Los Alamos Scientific Laboratory
P. O. Box 1663
Los Alamos, New Mexico 87344
    Attn:  Library
           D. Forslund
           J. Kindell
           B. Bezzerides
           D. Dubois
           H. Dreicer
           J. Ingraham
           R. Boyer
           C. Nielson
           E. Lindman
           L. Thode
           B. Godfrey

N.O.A.A.
325 Broadway S.
Boulder, Colorado 80302
    Attn:  J. Weinstock
           Thomas Moore (SEL,R-43)
           W. Bernstein
           D. Williams

Oak Ridge National Laboratory
P. O. Box V
Oak Ridge, Tennessee 37830
    Attn:  I. Alexeff
           C. Beasley
           D. Swain
           D. Spoug

Sanda Laboratories
Albuquerque, New Mexico 87115
    Attn:  A. Toepfer
           G. Yeonas
           D. VanDevender
           J. Freeman
           T. Wright

Austin Research Association
600 W. 28th Street
Austin, Texas 78705
    Attn:  J. R. Thompson
           L. Sloan

Bell Laboratories
Murray Hill, New Jersey 07974
    Attn:  A. Hasegawa

Lockheed Research Laboratory
Palo Alto, California 94304
    Attn:  M. Walt
           J. Cladis

Maxwell Laboratories
9244 Balboa Avenue
San Diego, California 92123
    Attn:  A. Kolb
           A. Mondelli
           P. Korn

Physics International Co.
2400 Merced Street
San Leandro, California 94577
    Attn:  J. Benford
           S. Putnam
           S. Stallings
           T. Young

Science Applications, Inc.
Lab. of Applied Plasma Studies
P. O. Box 2351
LaJolla, California 92037
    Attn:  L. Linson
           J. McBride

Goddard Space Flight Center
Greenbelt, Maryland 20771
    Attn:  M. Goldstein
           T. Northrup

Wu, Ching Sheng
Inst. of Physical Sci. and Tech.
University of Maryland
College Park, Maryland 20742

Matthews, David
IPST
University of Maryland
College Park, Maryland 20742

Zanetti, Lawrence
Applied Physics Lab.
SIP/Johns Hopkins Road
Laurel, Maryland 20810

# END

## DATE
## FILMED

12-81

## DTIC